Reprinted from the American Ceramic Society Bulletin, Vol. 66, No. 4, April 1987

Am. Ceram. Soc. Bull., **66** [4] 656–63 (1987)

Multinuclear Magic-Angle Sample-Spinning Nuclear Magnetic Resonance Spectroscopic Studies of Crystalline and Amorphous Ceramic Materials

GARY L. TURNER,* R. JAMES KIRKPATRICK,* SUBHASH H. RISBUD,* and ERIC OLDFIELD

University of Illinois, Urbana, IL 61801

Nuclear magnetic resonance (NMR) spectroscopy using magic-angle sample-spinning (MASS) techniques is a powerful tool for determining the local structural environment of a wide variety of elements in both crystalline and amorphous materials. It is useful for determining the phases present in a sample and the structure (including order/disorder) of such phases and for following the course of reactions at the atomic level. Applications of the MASS NMR method to ceramic materials are discussed. Some of the published data for materials of ceramic interest are reviewed. Some new results for such systems are provided. Nuclides discussed include ^{11}B, ^{15}N, ^{27}Al, ^{29}Si, and ^{31}P.

The local structure of amorphous oxidic and nonoxidic ceramic systems is a subject of considerable importance in modern materials science. Structural studies of a wide variety of glasses, ceramics, and semiconducting materials of aluminate, silicate, germanate, borate, chalcogenide, and fluoride compositions have been published. Topological modeling approaches, Raman and ir spectroscopy, neutron diffraction, X-ray radial distribution functions, extended X-ray absorption fine structure (EXAFS), and molecular dynamics simulations are among the many methods directed toward probing the long and short range structures of such systems. With the rapid development of unconventional processing methods for ceramics production (e.g. rapid solidification, sol-gel synthesis, and high pressure compaction), there is a growing awareness that the structure of a material is significantly related to its mode of formation and to its subsequent transformations.

The present paper discusses the application of "magic-angle" sample-spinning nuclear magnetic resonance (MASS NMR) spectroscopy to ceramic materials. Although NMR techniques for investigating liquids have been used for many years, it is only in the last 5 or 6 yr that high resolution NMR spectroscopic techniques have become popular for examining the local structural environment of a wide range of nuclei in solid samples. These techniques have proven to be of particular importance in examining the structures of fine grained and amorphous materials that cannot be effectively examined by single crystal diffraction (or NMR) methods.

The present paper briefly reviews the theory of MASS NMR of solids, describes the instrumentation needed, presents experimental results and interpretations for a number of nuclides in glasses and crystals of technological interest, and discusses future prospects for application of the method. The nuclides for which data are presented and discussed include ^{11}B, ^{15}N, ^{27}Al, ^{29}Si, and ^{31}P.

Theoretical Background

An elementary but fairly complete introduction to NMR theory is given by Davis.[1] More advanced treatments are given by Akitt,[2] Farrar and Becker,[3] Becker,[4] and Abragam.[5] Fyfe[6] provides an excellent and extensive treatment of MASS NMR. Brief summaries of the theory necessary to understand MASS NMR of solids and of the experimental methods are presented in articles by Lippmaa *et al.*,[7] Samoson *et al.*,[8] Müller *et al.*,[9] Smith *et al.*,[10] and Kirkpatrick *et al.*[11] Oldfield and Kirkpatrick[12] have presented a short summary of MASS NMR theory and recent results.

The following summarizes the most important points needed to understand MASS NMR. (1) Many atomic nuclei possess a quantized property called spin, characterized by the nuclear spin quantum number, I. Application of a static magnetic field, H_0, removes the degeneracy of the nuclear spin energy levels, giving rise to $2I+1$ such levels. For example, if $I=½$, the nucleus has $(2\times½)+1=$two energy levels and behaves as a magnetic dipole. If $I\geq1$, the nucleus has more than two energy levels and behaves as a magnetic quadrupole. (2) The NMR experiment measures the frequency of the radio frequency radiation which has the correct energy to cause transitions from one nuclear spin state to another. (3) The frequency that causes this transition, for a particular set of energy levels and for a particular nuclide, depends primarily on the magnitude of H_0 but varies a small amount from one chemical environment to another because electrons in the vicinity of the nucleus shield it to varying degrees from the applied magnetic field. These resonance frequencies are reported as deviations from an experimentally useful standard and are called *chemical shifts*. They are generally small, of the order of a few parts per million, but can be as large as several thousand parts per million for the heaviest elements. More positive chemical shifts correspond to higher frequency absorptions and correlate with less shielding (i.e., the nuclei "see" a larger value of the external magnetic field, H_0, thus resonate at a higher frequency). (4) For crystalline

*Member, the American Ceramic Society.

Received February 3, 1986; revised copy received July 10, 1986; approved October 17, 1986.

Supported in part by the National Science Foundation Solid-State Chemistry Program (Grant No. DMR 83-11339 and Grant No. DMR86-15206) and by the NSF Ceramics and Electronics Materials Program (Grant No. DMR 84-04013).

Peer Reviewed Contribution

materials under MASS conditions, nuclides with $I=½$, such as ^{13}C, ^{15}N, ^{29}Si, and ^{31}P, yield narrow peaks at the true, isotropic chemical shift value. (5) Quadrupolar nuclides ($I\geq1$, such as ^{11}B, ^{17}O, ^{23}Na, ^{25}Mg, and ^{27}Al) often yield peaks that are broadened and split by quadrupolar interactions and are often displaced from the isotropic value. The magnitudes of these effects are controlled by the nuclear quadrupole coupling constant (QCC) and the asymmetry parameter (η) of the electric field gradient tensor at the nucleus. For quadrupolar nuclides, usually only the central $(1/2, -1/2)$ transition is observed because the rest of the spectrum is exceedingly broad due to the quadrupolar interaction. The quadrupole interaction does not affect the central $(1/2, -1/2)$ transition to first order since it behaves as a pseudospin $-1/2$ particle.

For solids examined under nonspinning conditions, a variety of magnetic interactions may greatly broaden the peaks. However, peaks almost as narrow as for solutions ($\lesssim$1 ppm) can often be obtained for nuclei having $I=1/2$ by spinning the sample (usually 50–200 mg of powder) at kilohertz frequencies about an axis oriented at 54.7° to the (H_0) magnetic field direction ("magic-angle" sample-spinning, MASS; see Andrew[13]). This is because the equations describing most of these interactions (under MASS conditions) contain terms involving $3\cos^2\theta-1$, where θ is the angle between H_0 and the axis of rotation. This term reduces to zero when $\theta=54.7°$. Magic-angle sample-spinning averages the orientation-dependent contributions to the chemical shielding (found in powders), as well as the dipole-dipole interaction between nuclei and the first-order quadrupole interaction. However, if the QCC is very large, then second-order quadrupolar broadening effects become significant, and these residual broadenings remain in the MASS spectrum and are only partially averaged by sample-spinning. If the orientation-dependent chemical shielding is very large, then characteristic "powder pattern" lineshapes may be observed for nonspinning samples, reflecting the principal elements of the chemical shift tensor ($\delta_{11},\delta_{22},\delta_{33}$). Magic-angle sample-spinning at rates less than the overall breadth of this interaction causes formation of spinning sidebands, the intensities of which yield the elements of the chemical shift tensor. If the interaction is small, only the isotropic chemical shift (equal to $1/3(\delta_{11}+\delta_{22}+\delta_{33})$) is observed, as with the case of nonspinning samples. However, in both situations the use of MASS gives improved (peak) signal-to-noise ratios due to the collapse or narrowing of broad static lineshapes and frequent removal of both chemical shift and dipolar interactions.

There is, at present, no simple and precise way of theoretically calculating the magnitude of the chemical shift for a particular known (or assumed) local structural environment. Thus, because chemical shifts cannot be readily calculated, most recent work has involved examining the MASS NMR behavior of structurally and chemically well known phases in order to provide a database from which to interpret the spectra of less well characterized materials in a more-or-less empirical fashion. The variations in the reasonance frequencies (chemical shifts) of a particular nuclide in solids appear to be due primarily to nearest-neighbor (NN) and next-nearest-neighbor (NNN) interactions. It is this reason that makes NMR such a powerful technique for examining the *local* structural environment of atoms, even in, for instance, Al/Si disordered crystals and glasses.

Modern NMR spectrometers determine the resonance frequency by detecting the radio frequency emission from a sample in which the population of nuclei in the higher energy spin-state has been raised by absorption of a few-microsecond-long burst of radio frequency radiation at the resonance frequency. The emitted radiation is detected in the so-called time domain (intensity vs time), and the signal is then Fourier transformed into the frequency domain (intensity vs frequency) to yield the NMR spectrum. This is referred to as the pulsed Fourier transform NMR approach. A much higher signal-to-noise ratio is usually obtained with this method than with the older continuous wave methods which have been used to examine glass structure[14] because of the multichannel advantage of the Fourier transform method, which arises because both signal and noise are simultaneously monitored (as opposed to occasionally scanning through a peak). The Fourier advantage is lost, however, when only a single peak is present in the spectrum. A high field continuous wave approach would appear most attractive for studies of extremely broad lines in ceramic materials, but unfortunately such instruments are not commercially available.

A modern NMR spectrometer consists of a high field magnet (now mostly superconducting solenoids); electronics for generating the radiofrequency pulses that excite the nuclei into higher energy spin states (basically, an amateur radio transmitter); a sample-containing probe (a simple LC circuit); electronics for detecting the radiofrequency emission from the sample (a radio receiver); and a computer and disk system for controlling the electronics and processing, plotting, and storing the NMR data. The sample is held inside the magnet by a "probe" which contains the sample-spinning apparatus, an antenna coil used for transmitting rf to and from the sample, and capacitors to tune the circuit to resonance. Spectrometers can be purchased commercially (approximately $200 000 to $700 000), or can be "home-built" at less cost. Field strengths of currently available MASS NMR spectrometers range from 2.3T (100 MHz ^1H resonance frequency) to 11.7 T (500 MHz ^1H resonance frequency). Instruments operating in the range 600 to 900 MHz are likely to become available in the next 5 yr, although the very highest field instruments will likely cost in excess of $1.0 million.

Results And Discussion

Spin $I=1/2$ Nuclides

Nuclides with nuclear spin $I=1/2$ normally yield the most easily interpreted spectra because all linebroadening interactions are averaged by MASS. In particular, there are no quadrupolar effects to broaden and distort the peaks. However, spectra of the intrinsically most sensitive ^1H and ^{19}F nuclei are difficult to obtain in solids, because they often have large dipole-dipole interactions, which can only be removed at the highest spinning speeds or by application of more difficult multiple-pulse techniques. Spectra and spectral interpretations are presented here for the spin $I=1/2$ nuclides ^{15}N, ^{29}Si, and ^{31}P, which are readily obtained even at low magnetic field strengths, although high field operation facilitates determination of the individual elements of the chemical shielding tensor and provides enhanced sensitivity.

Silicon-29 Because of its importance and relative experimental simplicity, ^{29}Si has been the most investigated nuclide in inorganic solids, and for silicates a great deal is now understood about the relationships between the ^{29}Si chemical shift and Si-O-(Si,Al) bond angles, Si-O bond distances, polymerization state, number of Al NN and NNN and NNN bond strengths, band gap magnitudes,[15] and NN and NNN group electronegativities.[16] This work on silicates has recently been reviewed by Mägi *et al.*,[17] Kirkpatrick *et al.*,[11] and by Oldfield and Kirkpatrick.[12] The present paper will concentrate instead on silicate glasses, mixtures of glasses and crystals, carbides, nitrides, and oxynitride ceramics.

Figure 1 presents ^{29}Si MASS NMR spectra of a variety of crystalline, partially crystalline, and amorphous materials. The spectrum of α-SiC (Fig. 1(A)) contains three peaks and illustrates the point that different electronic environments for a given element, even in the same material, can give rise to NMR peaks at different chemical shifts. For 6H SiC all Si atoms are four-

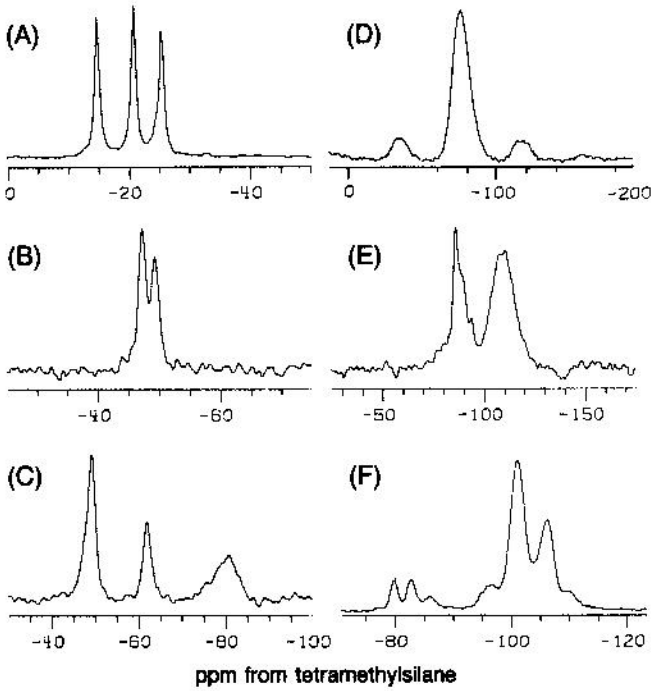

Fig. 1. ^{29}Si NMR spectra at 8.45 T: (A) α-SiC, 3.0 kHz MASS, 200 scans, 2 μs pulse length, 10 s recycle time, 50 Hz exponential linebroadening, spectral window=3.6 kHz; (B) $Si_3{}^{15}N_4$, 3.2 kHz MASS, 356 scans, 6 μs pulse length, 30 s recycle time, 10 Hz exponential linebroadening, spectral window=3.6 kHz; (C) $Si_3{}^{15}N_4$, $Si_2{}^{15}N_2O$ mixture, 3.5 kHz MASS, 305 scans, 6 μs pulse length, 30 s recycle time, 10 Hz exponential linebroadening, spectral window=5 kHz; (D) Na_2O (46%)·Al_2O_3(12.5%)·SiO_2(41.5%), 2.9 kHz MASS, 387 scans, 3 μs pulse length, 120 s recycle time, 10 Hz exponential linebroadening, spectral window=10.7 kHz; (E) mullite-SiO_2 mixture, 2.5 kHz MASS, 1810 scans, 2.3 μs pulse length, 10 s recycle time, 50 Hz exponential linebroadening, spectral window=10.8 kHz; (F) cordierite-forsterite, 2.7 kHz MASS, 1075 scans, 4 μs pulse length, 60 s recycle time, 50 Hz exponential linebroadening, spectral window=10.7 kHz.

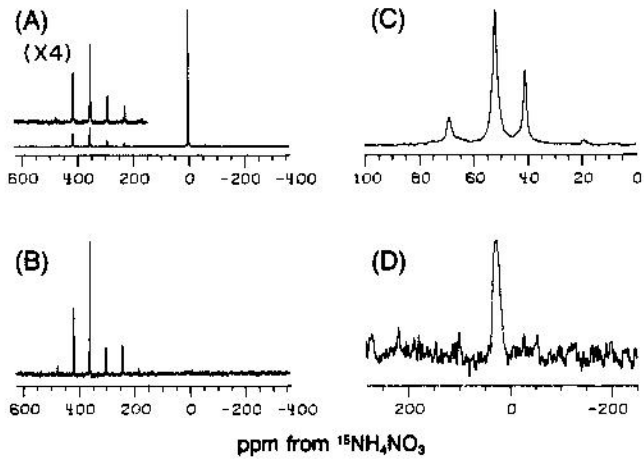

Fig. 2. ^{15}N NMR spectra at 11.7 T. For all, 3 μs pulse length, 120 s recycle time. (A) $^{15}NH_4{}^{15}NO_3$, 3.1 kHz MASS, 72 scans, 20 Hz exponential linebroadening, spectral window=50 kHz; (B) $K^{15}NO_3$, 3.0 kHz MASS, 58 scans, 20 Hz exponential linebroadening, spectral window=50 kHz; (C) $Si_3{}^{15}N_4$, $Si_2{}^{15}N_2O$ mixture, 3.9 kHz MASS, 300 scans, 20 Hz exponential linebroadening, spectral window=5 kHz; (D) MgSiAlO^{15}N, 3.9 kHz MASS, 664 scans, 100 Hz exponential linebroadening, spectral window=27 kHz.

coordinated by C atoms. Finlay *et al.*[18] have attributed these three peaks to three different NNN structural environments for Si and have also demonstrated that the three NNN environments to C in 6H SiC give rise to three ^{13}C NMR peaks.

Figure 1(B) presents the ^{29}Si spectrum of Si_3N_4 and shows two partially resolved peaks, which presumably arise from the α and β polymorphs. Figure 1(C) presents the ^{29}Si spectrum of Si_3N_4 and Si_2N_2O (along with unreacted elemental Si) produced by reacting $^{15}N_2$ gas with Si at 1450°C in an SiO_2 glass tube. Silicon nitride has the least shielded signal and Si the most. Because ^{29}Si does not suffer from quadrupolar interactions, if care is taken to allow the ^{29}Si nuclear spin system to fully relax between pulses, peak areas in such spectra are directly proportional to the total number of Si atoms in each phase. These two spectra show clearly that Si in an oxynitride environment can be readily distinguished from that in a nitride environment.

Figure 1(D) presents a ^{29}Si spectrum of an Na_2O-Al_2O_3-SiO_2 glass with a relatively high Na content and illustrates the point that for most glasses the ^{29}Si peaks are broad and essentially structureless. Well-resolved ^{29}Si peaks are observed for only a few Li- and Na-silicate glasses, which may be phase separated.[19-21] In general, the increased breadth of the peaks for glasses relative to those for crystals is due to an increased number of types of Si sites in the glasses, together with a broad range of bond angles and bond distances for each type of site.[22] Despite the lack of resolution in the ^{29}Si spectra of glasses, the average chemical shift, as measured by the position of the peak maximum, becomes more shielded (more negative) with increasing Si/(Si+Al) ratio and increasing average polymerization, paralleling the variations found for crystalline silicates.[23]

Silicon-29 MASS NMR is also useful for detecting the presence of glass and crystalline phases in a composite sample, in identifying the crystalline phases, and in determining something about the glass structure and composition. Figure 1(E) is the ^{29}Si spectrum of a partially devitrified glass with the composition $58SiO_2 \cdot 42Al_2O_3$, cooled from above the liquidus at ≈100°C/min. The spectrum consists of a relatively narrow peak at −87.0 ppm, due to crystalline mullite, and a broader peak at −108.3 ppm, due to a nearly pure SiO_2 glass (pure SiO_2 glass is at approximately −111 ppm). The peak for the mullite is relatively broad for a crystalline material, and the peak breadth may indicate the presence of overlapping signals from several sites.

Figure 1 is the ^{29}Si spectrum of crystalline cordierite. The peaks near −80 ppm are due to signal from the T1 Si sites in cordierite with from 1 to 4 Al next-nearest neighbors,[24] and the peaks between −90 to −110 ppm are due to a signal from the T2 Si sites of cordierite with from 1 to 4 Al next-nearest neighbors.[24]

Nitrogen-15 Nitride and oxynitride ceramics are important components of many refractory materials and glasses and are becoming increasingly important in many technological processes. Unfortunately, the only spin $I=1/2$ nitrogen nuclide is ^{15}N, which has a 0.37% natural abundance, and it can only be readily observed in costly, artificially ^{15}N-enriched samples. There is a considerable body of literature about ^{15}N NMR in solution and in organic solids, but there have been only a few studies of inorganic solids.[25-28]

Figure 2(A) is the ^{15}N MASS NMR spectrum of $^{15}NH_4{}^{15}NO_3$. The peak at 0 ppm arises from N in the ammonium group (which we use as the chemical shift standard, which is 358 ppm upfield of CH_3NO_2, another common ^{15}N reference material). The peak at 353 ppm from $^{15}NH_4NO_3$ arises from N in the nitrate group. The remaining peaks are spinning sidebands which,

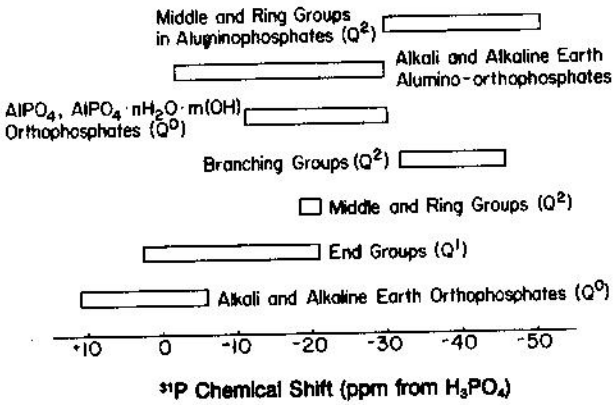

Fig. 3. Phosphorus-31 chemical shift ranges.

in this case, are associated with the nitrate peak. Figure 2(B) is an ^{15}N spectrum of $K^{15}NO_3$. The isotropic peak is at 358 ppm, and the remaining peaks are spinning sidebands. Thus, replacement of NH_4^+ by K^+ causes only a small ($\approx$5 ppm) change in chemical shift because the nitrate N is effectively isolated from the counterions by the three covalently attached oxygens. The N is, however, in a rather distorted (trigonal) environment in NO_3^-, whereas in the NH_4^+ ion it is at a center of high symmetry. As a result, the chemical shielding in the solid is markedly orientation-dependent for NO_3^-, but is essentially orientation-independent for the NH_4^+ ion. These effects can be quantitatively described by a chemical shift tensor, having components $\delta_{11}=448$ ppm, $\delta_{22}=411$ ppm, and $\delta_{33}=200$ ppm for $NH_4{}^{15}NO_3$, and $\delta_{11}=434$ ppm, $\delta_{22}=378$ ppm, and $\delta_{33}=264$ ppm for $K^{15}NO_3$. For $^{15}NH_4NO_3$, $\delta_{11}=\delta_{22}=\delta_{33}=\delta_{isotropic}=0$ ppm. Note that very small chemical shift tensors (i.e. $\delta_{11}\sim\delta_{22}\sim\delta_{33}$) are expected to be seen for any ion on a high symmetry site, e.g. $^{15}N^{3-}$, in a cubic material. Only if there are strongly directional bonds, as for example in NO_2^- or NO_3^-, are large chemical shift tensors expected to be seen.

Figure 2(C) is the ^{15}N MASS NMR spectrum of (enriched) $Si_3{}^{15}N_4$ and $Si_2{}^{15}N_2O$ made by reacting $^{15}N_2$ gas with elemental Si at 1450°C in a SiO_2 glass tube. The peak at 68.9 ppm is from an impurity, possibly MoN (perhaps formed by reaction of Mo or $MoSi_2$ vapor given off by the $MoSi_2$ heating elements). The shoulder at $\approx$57 ppm on the Si_3N_4 peak may be from the less abundant α-Si_3N_4 phase, while the main peak (at 51.6 ppm) probably arises from β-Si_3N_4. The peak at 40.6 ppm is from Si_2N_2O, and it is clear that the presence of oxygen around the NSi_4 tetrahedra increases the shielding at the N nucleus. As in the ^{29}Si spectrum of this sample, oxynitride and nitride environments are readily distinguished.

Figure 2(D) is the ^{15}N MASS NMR spectrum of a Mg-SiAlON glass, prepared by melt cooling an MgO-Al_2O_3-SiO_2-$Si_3{}^{15}N_4$ batch. The peak has a broad maximum at $\approx$27 ppm and, as with spectra of most nuclides in glasses, is broadened relative to those for crystals. The full width at half-height for the glass is $\approx$20 ppm, compared with only $\approx$1–2 ppm in the crystals. The N in this glass is clearly in a nitride or oxynitride structural environment, based on its close similarity in chemical shift to Si_3N_4/Si_2N_2O, and is clearly not present as nitrate, which should resonate several hundred parts per million away. Because the N content of this glass is low (batched at $\approx$10 wt%), the N is nonetheless likely to be in a very oxygen-rich environment. An alternative possibility is that all or part of the N may be coordinated to Al, as well as Si atoms. The ^{15}N chemical shift for AlN has not yet been recorded, and experiments with Al-free MgSiON glasses are in progress to clarify this point.

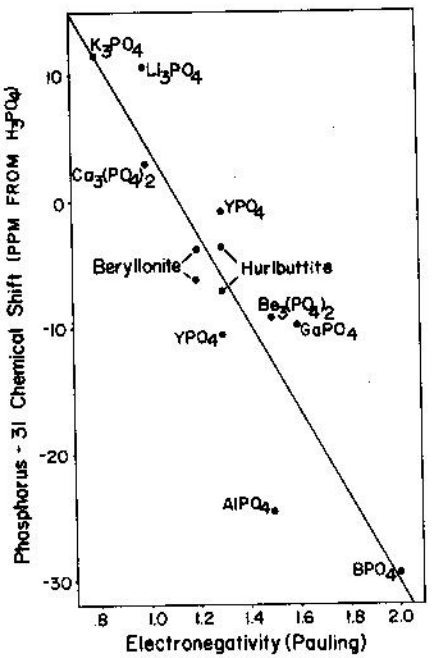

Fig. 4. Plot of ^{31}P chemical shift vs cation Pauling electronegativity for orthophosphates. The straight line represents the linear least-squares fit to the points.

The results presented here and elsewhere indicate that ^{15}N chemical shifts (currently) fall into the ranges 335 to 360 ppm for nitrate groups, 550 to 565 ppm for nitrite groups, $\approx$10 to 80 ppm for nitrides and oxynitrides, and are $\approx$0 ppm for ammonium groups. The range for nitrides is very likely to expand considerably as more data become available.

Phosphorus-31 Phosphorus is an important component in many glasses and crystalline or partially crystalline ceramic materials and in Al-phosphate and phosphosilicate catalysts and molecular sieves. The ^{31}P MASS NMR behavior of a number of systems has been described. These include: $AlPO_4$ molecular sieves,[29,30] polymerized (condensed) phosphates,[31,32] and orthophosphates.[33]

Phosphorus-31 chemical shifts fall into distinct ranges for different types of structural environment (Fig. 3). Overall, the variation parallels that observed with ^{29}Si. The shielding at P increases as polymerization increases,[31] and for orthophosphates, the shielding at P increases as the electronegativity of the NNN cation increases (Fig. 4).[33]

Figure 5 presents ^{31}P MASS NMR spectra of a representative selection of crystals and glasses. The spectra of crystalline $Na_3PO_4 \cdot 12H_2O$ and $AlPO_4$ (Figs. 5(A) and 5(B)) illustrate the typically narrow peaks obtained when investigating crystalline compounds. However, $NaPO_3$ glass (Figure 5(C)) yields a much broader ^{31}P resonance than crystalline $Na_3PO_4 \cdot 12H_2O$, and the isotropic chemical shift occurs at a more shielded value due to its greater polymerization. This latter spectrum may indicate that the dominant structural environment about P in the metaphosphate glass is the same as in the crystal (PO_4 groups containing bridging oxygens) but that there is a range of P–O bond lengths and O–P–O bond angles in the glass. Also notable is the large increase in chemical shift anisotropy in the polymerized state. The ^{31}P spectrum of a $CaSiO_3$ glass to which 2 wt% P_2O_5 has been added is also broader than a crystalline

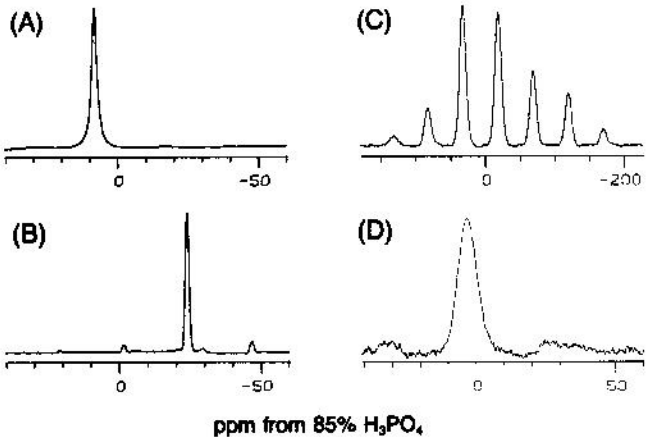

Fig. 5. ^{31}P MASS NMR spectra of phosphates at 8.45 and 11.7 T: (A) $Na_3PO_4 \cdot 12H_2O$, 4.8 kHz MASS, 124 scans, 3 μs pulse length, 10 s recycle time, 20 Hz exponential linebroadening, spectral window = 20 kHz, proton-decoupled; (B) $AlPO_4$, 4.6 kHz MASS, 20 scans, 4 μs pulse length, 10 s recycle time, 20 Hz exponential linebroadening, spectral window = 20 kHz; (C) $NaPO_3$ glass, 3.1 kHz MASS, 60 scans, 1 μs pulse length, 20 s recycle time, 100 Hz exponential linebroadening, spectral window = 2 kHz (The isotropic chemical shift is at −20.4 ppm; the other peaks are spinning side-bands.); (D) $CaSiO_3$ glass with 2 wt% P_2O_5, 3.1 kHz MASS, 9388 scans, 5 μs pulse length, 3 s recycle time, 50 Hz exponential linebroadening, spectral window = 14.5 kHz.

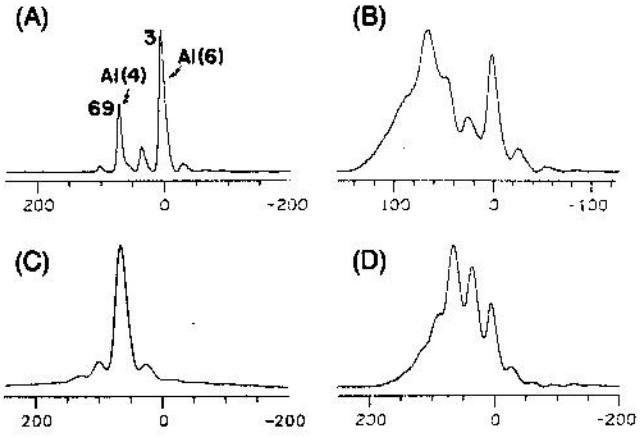

Fig. 6. ^{27}Al NMR spectra at 11.7 T: (A) Mixed-layer illite/smectite synthetic clay, 3.7 kHz MASS, 5876 scans, 12 μs pulse length, 1 s recycle time, 100 Hz exponential linebroadening, spectral window = 59 kHz; (B) synthetic mullite, 3.3 kHz MASS, 5824 scans, 4 μs pulse length, 1 s recycle time, 100 Hz exponential linebroadening, spectral window = 37 kHz; (C) $50CaO \cdot 8Al_2O_3 \cdot 42SiO_2$ glass, 4.5 kHz MASS, 358 scans, 2 μs pulse length, 1 s recycle time, 50 Hz exponential linebroadening, spectral window = 59 kHz; (D) $50Al_2O_3 \cdot 50SiO_2$ glass, 3.8 kHz MASS, 2000 scans, 2 μs pulse length, 0.5 s recycle time, 100 Hz exponential linebroadening, spectral window = 59 kHz.

phase of the same overall composition (Fig. 5(D)). The peak maximum is at the same position (+3 ppm from H_3PO_4) as $Ca_3(PO_4)_2$, suggesting that phosphorus in the glass does not enter the polymerized silicate structure but instead is present as calcium orthophosphate-like units. Phosphorus-31 MASS NMR, then, appears to be a potentially useful technique for determining the structural environment of P in a wide variety of materials, and plans are being made to obtain spectra of fluorophosphate glasses which are of current interest in glass-metal sealing.

Spin $I > 1/2$ Nuclides

Nuclides which have spin $I > 1/2$ have a nuclear quadrupole moment (eQ) that can interact with the electric field gradient at the nucleus (eq) to give a large broadening interaction characterized by the quadrupole coupling constant (QCC), e^2qQ/h. If the QCC is large, the peak for a given structural site can be broadened, displaced to more shielded values than the true (isotropic) chemical shift, and split and distorted into complicated shapes. The majority of nuclides which have a nonzero spin are quadrupolar, and therefore there is considerable interest in developing NMR techniques for analyzing these systems. Those that yield the most readily obtainable spectra are those with nonintegral spins ($I = 3/2, 5/2, 7/2, 9/2$), for which the central $(-1/2, 1/2)$ transition can be readily observed, because to first-order it behaves as a spin $I = 1/2$ nuclide and is not broadened by quadrupolar effects. However, as the quadrupole interaction becomes a significant fraction of the Zeeman interaction (the splitting of the otherwise degenerate energy levels due to application of the external magnetic field), the higher order terms can affect the lineshape. Specifically, the observed width and shape for large QCC values are dominated by the second-order quadrupole interaction.[12]

For a given QCC, the second-order broadening decreases as the magnetic field strength increases. Quantitatively, it can be shown for systems in which the second-order broadening dominates the linewidth that the spectral resolution (peak separation divided by peak width) increases as $(H_0)^2$. Thus, spectra of nonintegral spin quadrupolar nuclei should (usually) be collected at the highest magnetic field strengths possible. All spectra reported here were collected at $H_0 = 11.7$ (the largest commercially available field strength in a persistent magnet) unless otherwise specified. Care should be taken when comparing chemical shifts of quadrupolar nuclei obtained at different magnetic field strengths because of the potential displacement of the peak position due to the second-order quadrupole interaction. Kirkpatrick *et al.*[11] and Kinsey *et al.*[34] have illustrated the effects of field strength on the ^{23}Na and ^{27}Al MASS NMR spectra of crystalline aluminosilicate materials. If quadrupole coupling constant information is required for sites having very small e^2qQ/h values, *low field* operation is preferable, since the magnitude of the second-order broadening is inversely proportional to the applied field strength.

Aluminum-27 Aluminum-27 is the most thoroughly investigated quadrupolar nuclide in inorganic solids. Aluminum-27 MASS NMR has found application in examining, for example, zeolite catalysts and molecular sieves, clay minerals, glasses, and aluminas. The variation of the ^{27}Al chemical shift with structure and composition in crystalline aluminosilicates has been discussed by Kirkpatrick *et al.*[35]

One of the most important uses of ^{27}Al MASS NMR is the detection of four-coordinated (Al(4)) and six-coordinated (Al(6)) Al, which is usually an easily made distinction. Figure 6(A) is the ^{27}Al MASS NMR spectrum of a synthetic clay (mixed-layer illite/smectite) showing the presence of peaks for Al(4) at 69 ppm and Al(6) at 3 ppm. For oxides and aluminosilicates, the ^{27}Al chemical shifts for Al(4) fall into the range of $\approx$45 to 80 ppm, and those for Al(6) fall into the range of about −10 to +15 ppm.

For aluminosilicates, the Al(4) chemical shift becomes less shielded (more positive) with decreasing Si/(Si+Al(4)). The ^{27}Al chemical shift of Al(4) with four bridging oxygens is more

shielded than that of Al(4) with three bridging oxygens by ≈10–15 ppm at the same Si/(Si+Al(4)) ratio.

Figure 6(B) is a ^{27}Al MASS NMR spectrum of a synthetic mullite, showing peaks for Al(4) at ≈64 ppm and Al(6) at ≈0 ppm, and an additional small peak at ≈44 ppm. The peak at 44 ppm could arise from Al(4) in triclusters. These Al atoms are coordinated to oxygen, which is three-coordinated by Al(4),[36] which could cause an increased shielding of the Al atoms coordinated to it. However, additional experiments at much higher spinning-speeds will be required in order to rule out the possibility that this peak arises from spinning side-bands.

Aluminum-27 NMR is also a powerful tool for determining the structural state of Al in glasses and gels. A number of papers[23,37-43] have investigated the ^{27}Al MASS NMR behavior of various amorphous aluminosilicates. Figure 6(C) shows the ^{27}Al spectrum of a $50CaO \cdot 8Al_2O_3 \cdot 42SiO_2$ glass. Although the peak is somewhat broader than that for aluminosilicate crystals, the peak position clearly indicates that only Al(4), with four bridging oxygens, is observable. The results of additional experiments indicate that all ^{27}Al in this glass (±10%) may be accounted for, i.e., there is no evidence for any significant quantities of Al(6).

Figure 6(D) is the ^{27}Al MASS NMR spectrum of a 50:50 mol% Al_2O_3/SiO_2 glass, made by rapidly quenching a melt between two liquid-N_2-cooled Ti rollers. The spectrum clearly indicates the presence of both Al(4) at 63 ppm and Al(6) at 3 ppm. The peak at 33 ppm in this case is most likely due to pentahedrally coordinated Al.

The ^{27}Al MASS NMR results available to date indicate that glasses and gels with molar ratios of modifier oxide/$Al_2O_3 \geq 1$ contain only Al(4), and that most of that is in Q^4 sites.[23] Amorphous materials with greater amounts of Al_2O_3 generally exhibit some peak intensity in the vicinity of 0 ppm, indicative of Al(6). For $NaAlSi_3O_8$ glass, Ohtani *et al.*[43] have recently used ^{27}Al MASS NMR to demonstrate the appearance of Al(6) in samples subjected to pressures >6 GPa.

Aluminas have also been investigated to some extent by ^{27}Al MASS NMR.[44-46] These studies clearly show the presence of only Al(6) in the Al_2O_3 precursors gibbsite and bayerite, the appearance of Al(4) on heating the precursors in the temperature range 400°–800°C, the presence of both Al(4) and Al(6) in the transitional aluminas, and the presence of only Al(6) in α-Al_2O_3 (corundum). Note that quantitatively reliable estimates of the actual percentages of the ^{27}Al observed in most of the NMR experiments cited above have not yet been reported, although they are certainly feasible.

Boron-11 Like Al, B is commonly present in solids in two different coordination states, in this case trigonal, B(3), and tetrahedral, B(4). Boron-11 MASS NMR can readily distinguish these two coordination environments and determine their relative abundances. As for ^{27}Al, the largest H_0 magnetic field strengths give the best resolution. Boron-11 NMR using wideline methods was pioneered by P. J. Bray and has been a most important method for examining the structure of borate and borosilicate glasses for many years.[47]

However, few laboratories are currently equipped with low field, continuous-wave NMR instruments, so some typical high field ^{11}B MASS NMR spectra are presented below. The principal advantage over the earlier work is that isotropic chemical shifts may be obtained for B(3) and B(4), although the shift ranges for each are small. A disadvantage of the ^{11}B MASS NMR method is that the QCC parameters for the (very narrow) B(4) sites are difficult to obtain at high field. However, this may be remedied in some instances by means of ^{10}B MASS NMR (data not shown).

Turner *et al.*[48] have examined the ^{11}B MASS NMR behavior of a variety of borate and borosilicate crystals and glasses. Figure 7 presents ^{11}B spectra and computer lineshape simulations

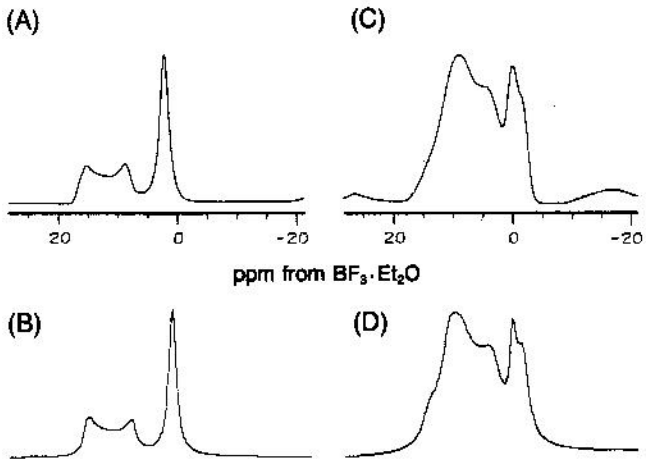

Fig. 7. ^{11}B NMR spectra at 11.7 T together with their computer simulations. For both, spectral window=8 kHz. (A) $Li_2B_4O_7$, 6 kHz MASS, 256 scans, 2 μs pulse length, 1 s recycle time; (B) simulation of (A), B(3) parameters are QQC=2.5 MHz, isotropic chemical shift=17.9 ppm, relative ratio=1; B(4) parameters are: QCC≈0.2 MHz, isotropic chemical shift=1.7 ppm, relative ratio=1; (C) commercial pyrex glass, 4.2 kHz MASS, 256 scans, 2 μs pulse length, 1 s recycle time; (D) simulation of (C), B(3) (low field signal) parameters are QQC=2.3 MHz, isotropic chemical shift=16.0 ppm, relative ratio=2. B(3) (high field signal) parameters are QCC=2.55 MHz, isotropic chemical shift=12.6 ppm, relative ratio=6. B(4) (low field signal) parameters are QCC≈0.5 MHz, isotropic chemical shift=1.8 ppm, relative ratio=1. B(4) (high field signal) parameters are QCC=0.5 MHz, isotropic chemical shift=0.2 ppm, relative ratio=1.

of some of these materials. Figure 7(A) is of $Li_2B_4O_7$ and shows the presence of B(3) and B(4). The simulation (Fig. 7(B)) indicates that two sites are present in a 1:1 ratio, in agreement with X-ray diffraction data and general compositional rules. The B(4) site yields a narrow, unsplit peak because of a low QCC (≈0.2 MHz), indicating a highly symmetric site. The B(3) site, however, is less symmetrical, has a QCC of ≈2.5 MHz and consequently yields a broadened and split peak. Such observations are not new. However, the isotropic chemical shifts of 17.9±0.2 ppm (from $BF_3 \cdot Et_2O$) for B(3) and 1.7±0.2 ppm for B(4) are, and further studies of these isotropic chemical shifts may augment our understanding of borate (glass) structures.

Figs 7(C) and 7(D) show the observed and simulated spectra of a pyrex glass (commercial glassware) and demonstrate that two B(3) and two B(4) sites are present. The relative abundances are: B(3), 60%; B(3), 20%; B(4), 10%; and B(4), 10%. The more shielded B(3) site and the more shielded B(4) site are tentatively interpreted as due to the effect of Si(4) substituting for B(3) in the NNN coordination shell, an effect which is quite large (≈4 ppm) for ^{11}B(4) in reedmergnerite.[48]

Future Prospects

Because high field NMR spectrometers can detect signals from such a wide range of nuclides, the technique is likely to find rapidly increasing application in examining the local structural environments present in many kinds of materials of current technological interest. Table I lists the nuclides that are likely candidates for NMR spectroscopy of solids, their spin, the difficulty of the experiment, and the type of experiment most easily used to examine it.

In addition, MASS NMR itself seems likely to become a

Table I. Some Nuclei of Potential Use in NMR Studies of Ceramics

Nucleus	Readily observed	Spin	Abundance	Frequency (11.7 T)	Technique*
H-1	yes	1/2	99.985	500	CRAMPS
Li-7	yes	3/2	92.58	194.3	MASS
Be-9	yes	3/2	100	70.3	MASS
B-10	yes	3	19.58	53.7	MASS
B-11	yes	3/2	80.42	160.4	MASS
C-13	yes	1/2	1.1	125.7	MASS/LABEL
N-14	yes	1	99.6	36.1	MASS/ECHO
N-15	yes	1/2	0.37	50.7	MASS/LABEL
O-17	yes	5/2	0.037	67.8	MASS/STATIC/LABEL
F-19	yes	1/2	100	470.4	MASS/CRAMPS
Na-23	yes	3/2	100	132.3	MASS/ECHO
Mg-25	yes	5/2	10.1	30.6	ECHO
Al-27	yes	5/2	100	130.3	MASS
Si-29	yes	1/2	4.7	99.3	MASS
P-31	yes	1/2	100	202.4	MASS
S-33	no	3/2	0.76	38.4	ECHO/LABEL
Cl-35	yes	3/2	75.5	49.0	MASS†
K-39	yes	3/2	93.1	23.3	ECHO
Sc-45	yes	7/2	100	121.5	ECHO
Ti-49	no	7/2	5.5	28.2	LABEL/ECHO
V-51	yes	7/2	99.76	131.4	MASS
Cu-63	yes	3/2	69.1	132.5	ECHO
Zn-67	yes	5/2	4.1	31.3	ECHO/LABEL
Ga-71	yes	3/2	39.6	152.5	MASS/ECHO
Ge-73	yes	9/2	7.8	17.4	ECHO
Se-77	no	1/2	7.6	95.3	MASS
Br-79	yes	3/2	50.5	125.3	MASS†
Rb-85	yes	5/2	72.15	48.3	ECHO†
Sr-87	no	9/2	7.0	21.7	ECHO†
Y-89	yes	1/2	100	24.5	MASS
Zr-91	no	5/2	11.2	46.7	ECHO†
Nb-93	yes	9/2	100	122.2	ECHO
Mo-95	yes	5/2	15.7	32.6	MASS/ECHO†
Ag-109	yes	1/2	48.18	23.3	MASS
Cd-113	yes	1/2	12.26	110.9	MASS
In-115	yes	9/2	95.72	109.6	ECHO
Sn-119	yes	1/2	8.58	186.4	MASS
Te-125	no	1/2	6.99	158.0	MASS
Cs-133	yes	7/2	100	65.6	MASS/ECHO
Ba-137	no	3/2	11.3	55.6	ECHO†
La-139	yes	7/2	99.9	70.6	ECHO
Yb-171	no	1/2	14.3	88.1	MASS
W-183	yes	1/2	14.4	20.8	MASS
Pt-195	no	1/2	33.8	107.5	MASS
Hg-199	yes	1/2	16.8	89.1	MASS
Ti-205	yes	1/2	70.5	288.5	MASS
Pb-207	yes	1/2	22.6	104.6	MASS

*Acronyms as follows: CRAMPS, Combined Rotation and Multiple-Pulse Spectroscopy[51]; MASS/LABEL, magic-angle sample-spinning on an isotopically *enriched* sample; STATIC, stationary sample; ECHO, use of one of the spin-echo methods described in Refs. 49 or 50, rather than MASS, is advised, because expected linewidths are large. †Little data available, but method proposed is probably effective.

useful quantitative tool for following the course of reactions at the atomic level. Thus, phase transformations, prenucleation phenomena, crystallization mechanisms, glass-in-glass immiscibility, and precipitation should all be amenable to investigation. Currently interesting problems in the nature of ceramic-metal interfaces, reactions of ceramic and glass surfaces with liquids and gases, and development of composites and electronic packaging materials are also well suited for structural study using these and related novel NMR techniques.[49,50] Finally, and most speculatively, while all of the systems studied to date have consisted of bulk crystals or powders, adequate spectrometer sensitivity should soon become available in order to observe molecules on single crystal surfaces. While such experiments will be difficult and time-consuming, the possibilities of investigating various adlayers on, for example, Si(111) seem real and could be of considerable interest in, for example, studying semiconductor manufacturing processes.

Acknowledgments

The authors thank Dr. Karen Smith for very useful discussion and Mr. Wang-Hong Yang for the use of his ^{31}P spectrum of P-doped $CaSiO_3$ glass.

References

[1]J. C. Davis, Advanced Physical Chemistry. Roland, New York, 1965.

[2]J. W. Akitt, NMR and Chemistry: An Introduction to the Fourier Transform-Multinuclear Era, 2d ed. Chapman and Hall, London, 1983.

[3]T. C. Farrar and E. D. Becker, Pulse and Fourier Transform NMR: Introduction to Theory and Methods. Academic Press, New York, 1971.

[4]E. D. Becker, High Resolution NMR: Theory and Application, 2d ed. Academic Press, New York, 1980.

[5]A. Abragam, The Principles of Nuclear Magnetism. Clarendon Press, Oxford, 1983.

[6]C. A. Fyfe, Solid State NMR for Chemists. C.R.C. Press, Guelph, ON, Canada, 1983.

[7]E. Lippmaa, M. Mägi, A. Samoson, G. Engelhardt, and A.-R. Grimmer, "Structural Studies of Silicates by Solid-State High-Resolution ^{29}Si NMR," *J. Am. Chem. Soc.*, **102**, 4889–93 (1980).

[8]A. Samoson, E. Kundla, and E. Lippmaa, "High Resolution MAS-NMR of Quadrupolar Nuclei in Powders," *J. Magn. Reson.*, **49**, 350–57 (1982).

[9]D. Müller, W. Gessner, H.-J. Behrens, and G. Scheler, "Determination of the Aluminum Coordination in Aluminum-Oxygen Compounds by Solid-State High-Resolution ^{27}Al NMR," *Chem. Phys. Lett.*, **79**, 59–62 (1981).

[10]K. A. Smith, R. J. Kirkpatrick, E. Oldfield, and D. M. Henderson, "High-Resolution Silicon-29 Nuclear Magnetic Resonance Spectroscopic Study of Rock-Forming Silicates," *Am. Mineral.*, **68**, 1206–15 (1983).

[11]R. J. Kirkpatrick, R. A. Kinsey, K. A. Smith, D. M. Henderson, and E. Oldfield, "High Resolution Solid-State Sodium-23, Aluminum-27, and Silicon-29 Nuclear Magnetic Resonance Spectroscopic Reconnaissance of Alkali and Plagioclase Feldspars," *Am. Mineral.*, **70**, 106–23 (1985).

[12]E. Oldfield and R. J. Kirkpatrick, "High-Resolution Nuclear Magnetic Resonance of Inorganic Solids," *Science*, **227**, 1537–44 (1985).

[13]E. R. Andrew, "The Narrowing of NMR Spectra of Solids by High-Speed Specimen Rotation and the Resolution of Chemical Shift and Spin Multiplet Structures for Solids," *Nucl. Magn. Reson. Spectrosc.*, **8**, 1–39 (1971).

[14]P. J. Bray, F. Bucholtz, A. E. Geissberger, and I. A. Harris, "NMR Studies of the Structure of Non-Metallic Glasses," *Nucl. Instrum. Methods*, **199**, 1–15 (1982).

[15]J. A. Tossell, "Correlation of ^{29}Si Nuclear Magnetic Resonance Chemical Shifts in Silicates with Orbital Energy Differences Obtained from X-ray Spectra," *Phys. Chem. Miner.*, **10**, 137–41 (1984).

[16]N. Janes and E. Oldfield, "Prediction of Silicon-29 Nuclear Magnetic Resonance Chemical Shifts Using a Group Electronegativity Approach: Applications to Silicate and Aluminosilicate Structures," *J. Am. Chem. Soc.*, **107**, 6769–75 (1985).

[17]M. Mägi, E. Lippmaa, A. Samoson, G. Engelhardt, and A.-R. Grimmer, "Solid-State High-Resolution Silicon-29 Chemical Shifts in Silicates," *J. Phys. Chem.*, **88**, 1518–22 (1984).

[18]G. R. Finlay, J. S. Hartman, M. F. Richardson, and B. L. Williams, "^{29}Si and ^{13}C Magic Angle Spinning NMR Spectra of Silicon Carbide Polymorphs," *J. Chem. Soc. Chem. Commun.*, 159–161 (1985).

[19]C. M. Schramm, B.H.W.S. de Jong, and V. E. Parziale, "^{29}Si Magic Angle Spinning NMR Study on Local Silicon Environments in Amorphous and Crystalline Lithium Silicates," *J. Am. Chem. Soc.*, **106**, 4396–4402 (1984).

[20]R. Dupree, D. Holland, P. W. McMillan, and R. F. Pettifer, "The Structure of Soda-Silicate Glasses: A MASS NMR Study," *J. Non-Cryst. Solids*, **68**, 399–410 (1984).

[21]A.-R. Grimmer, M. Mägi, M. Hähnert, H. Stade, A. Samoson, W. Weiker, and E. Lippmaa, "High-Resolution Solid-State ^{29}Si Nuclear Magnetic Resonance Spectroscopic Studies of Binary Alkali Silicate Glasses," *Phys. Chem. Glasses*, **25**, 105–09 (1984).

[22]R. J. Kirkpatrick, T. Dunn, S. Schramm, K. A. Smith, R. Oestrike, and G. Turner, "Magic-Angle Sample-Spinning Nuclear Magnetic Resonance Spectroscopy of Silicate Glasses: A Review"; in Structure and Bonding in Noncrystalline Solids. Edited by G. E. Walrafen and A. Revesz. Plenum Press, New York, 1986.

[23]R. W. Oestrike, "Inferences on the Structure of Aluminosilicate Glasses: A High Resolution Solid-State Silicon-29 and Aluminum-27 Nuclear Magnetic Resonance Study"; Ph.D. Thesis, Dept. of Geology, University of Illinois, Urbana, 1985.

[24]C. A. Fyfe, G. C. Gobbi, J. Klinowski, A. Puntis, and J. M. Thomas, "Char-

Gary L. Turner

R. James Kirkpatrick

Subhash H. Risbud

Eric Oldfield

Gary L. Turner is president of Spectral Data Services, Inc., Champaign, IL. He received a B.S. from the University of Illinois in 1978 and a Ph.D. from the University of Arkansas in 1982. He conducted postdoctoral research at the University of Illinois before joining Spectral Data Services, Inc.

R. James Kirkpatrick is professor of geology at the University of Illinois, Urbana. He received an A.B. from Cornell University in 1968 and a Ph.D. from the University of Illinois in 1972. He was a postdoctoral fellow in geophysics at Harvard University during 1973–1975 and was an Overseas Fellow at Churchill College, Cambridge University, United Kingdom. His research interests include NMR spectroscopy of solids, mineral physics, nucleation and growth kinetics, and igneous petrology.

Subhash H. Risbud is a professor in the Dept. of Materials Science and Engineering at the University of Arizona, Tucson. He obtained his Ph.D. from the University of California, Berkeley in 1976. Prior to joining the Arizona faculty, he was with the University of Illinois; Lehigh University; GTE, Wesgo Div.; and Stanford University. His research interests are in novel glasses and ceramics, electronic and optical materials, and ceramic-metal interface structures.

Eric Oldfield is a professor of chemistry at the University of Illinois, Urbana, whose faculty he joined in 1975. He was a European Molecular Biology Fellow at Indiana University from 1972 to 1974, and then a visiting scientist at the Massachusetts Institute of Technology, Cambridge. He was an undergraduate at Bristol University and a graduate student at Sheffield University in the United Kingdom. His interests include NMR spectroscopic studies of inorganic solids and assorted biological systems.

acterization of Local Atomic Environments and Quantitative Determination of Changes in Site Occupancies During the Formation of Ordered Synthetic Cordierite by ^{29}Si and ^{27}Al Magic-Angle Spinning NMR Spectroscopy," *J. Chem. Soc. Chem. Commun.*, 556–58 (1983).

[25]J. Mason, "Nitrogen Nuclear Magnetic Resonance Spectroscopy in Inorganic, Organometallic, and Bioinorganic Chemistry," *Chem. Rev.*, **81**, 205–27 (1981).

[26]M. G. Gibby, R. G. Griffin, A. Pines, and J. S. Waugh, "High Resolution NMR of ^{15}N in Solids," *Chem. Phys. Lett.*, **17**, 80–81 (1972).

[27]C. A. Fyfe, G. C. Gobbi, J. S. Hartman, R. E. Lenkinski, J. H. O'Brien, E. R. Beange, and M.A.R. Smith, "High-Resolution Solid-State MAS Spectra of ^{29}Si, ^{27}Al, ^{11}B and Other Nuclei in Inorganic Systems Using a Narrow-Bore 400-MHz High Resolution NMR Spectrometer," *J. Magn. Reson.*, **47**, 168–73 (1982).

[28]C. I. Ratcliffe, J. A. Ripmeester, and J. S. Tse, "^{15}N NMR Chemical Shifts in Solid NH_4^+ Salts," *Chem. Phys. Lett.*, **99**, 177–80 (1983).

[29]D. Müller, E. Jahn, G. Ladwig, and U. Haubenreisser, "High-Resolution Solid-State ^{27}Al and ^{31}P NMR: Correlation Between Chemical Shift and Mean Al-O-P Angle in $AlPO_4$ Polymorphs," *Chem. Phys. Lett.*, **109**, 332–36 (1984).

[30]C. S. Blackwell and R. L. Patton, "Aluminum-27 and Phsophorus-31 Nuclear Magnetic Resonance Studies of Aluminophosphate Molecular Sieves," *J. Phys. Chem.*, **88**, 6135–39 (1984).

[31]T. M. Duncan and D. C. Douglass, "On the ^{31}P Chemical Shift Anisotropy in Condensed Phosphates," *Chem. Phys.*, **87**, 339–49 (1984).

[32]E. R. Andrew, D. J. Bryant, E. M. Cashell, and B. A. Dunell, "Chemical Shift in Solid Sodium Triphosphate," *Chem. Phys. Lett.*, **77**, 614–17 (1981).

[33]G. L. Turner, K. A. Smith, R. J. Kirkpatrick, and E. Oldfield, "Structure and Cation Effect on Phosphorus-31 NMR Chemical Shifts and Chemical Shift Anisotropies of Model Orthophosphates," *J. Magn. Reson.*, **70**, 408–15 (1986).

[34]R. A. Kinsey, R. J. Kirkpatrick, J. Hower, K. A. Smith, and E. Oldfield, "High Resolution Aluminum-27 and Silicon-29 Nuclear Magnetic Resonance Spectroscopic Study of Layer Silicates, Including Clay Minerals," *Am. Mineral.*, **70**, 537–48 (1985).

[35]R. J. Kirkpatrick, K. A. Smith, S. Schramm, G. Turner, and W.-H. Yang, "Solid-State Nuclear Magnetic Resonance Spectroscopy of Minerals," *Ann. Rev. Earth Planet. Sci.*, **13**, 29–47 (1985).

[36]C. W. Burnham, "The Crystal Structure of Mullite," *Year Book Carnegie Inst. Washington*, **63**, 223–27 (1964).

[37]D. Müeller, D. Hoebbel, and W. Gessner, "^{27}Al NMR Studies of Aluminosilicate Solutions. Influences of the Second Coordination Sphere on the Shielding of Aluminum," *Chem. Phys. Lett.*, **84**, 25–29 (1981).

[38]J. M. Thomas, J. Klinowski, P. A. Wright, and R. Roy, "Probing the Environment of Al Atoms in Noncrystalline Solids: Al_2O_3-SiO_2 Gels, Soda Glass, and Mullite Precursors," *Angew. Chem. Int. Ed. Engl.*, **22**, 614–16 (1983).

[39]E. Hallas, U. Haubenreisser, M. Hähnert, and D. Müller, "NMR-Untersuchangen and Na_2O-Al_2O_3-SiO_2 Gläsern mit Hilfe der Chemischen Verschiebung von ^{27}Al-Kernen," *Glastech. Ber.*, **56**, 63–70 (1983).

[40]B.H.W.S. de Jong, C. M. Schramm, and V. E. Parziale, "Polymerization of Silicate and Aluminate Tetrahedra in Glasses, Melts, and Aqueous Solutions-IV. Aluminum Coordination in Glasses and Aqueous Solutions and Comments on the Aluminum Avoidance Principle," *Geochim. Cosmochim. Acta*, **47**, 1223–36 (1983).

[41]R. J. Kirkpatrick, K. A. Smith, R. Oestrike, C. A. Weiss, and E. Oldfield, "High-Resolution Aluminum-27 and Silicon-29 NMR Spectroscopy of Glasses and Crystals Along the Join $CaMgSi_2O_6$-$CaAl_2SiO_6$," *Am. Mineral.*, **71**, 705–11 (1986).

[42]C. A. Weiss and R. J. Kirkpatrick, "Aluminum-27 and Silicon-29 NMR Spectroscopy of Peraluminous Gels" (abstract), *EOS, Trans. Am. Geophys. Union*, **66**, 3956 (1985).

[43]E. Ohtani, F. Taulelle, and C. A. Angell, "Al^{3+} Coordination Changes in Liquid Aluminosilicates Under Pressure," *Nature (London)*, **314**, 78–81 (1985).

[44]V. M. Mastikhin, O. P. Krivoruchko, B. P. Zolotovskii, and R. A. Buyanov, "Study of Local Environment and Cation Distribution in Al(III) Oxides by ^{27}Al-NMR with Sample Rotation at a 'Magic' Angle," *React. Kinet. Catal. Lett.*, **18**, 117–20 (1981).

[45]C. S. John, N.C.M. Alma, and G. R. Hays, "Characterization of Transitional Alumina by Solid-State Magic Angle Spinning Aluminum NMR," *Appl. Catal.*, **6**, 341–46 (1983).

[46]R. A. Kinsey, "Solid State NMR of Quadrupolar Nuclei"; Ph.D. Thesis, Dept. of Chemistry, University of Illinois, Urbana, 1984.

[47]Y. H. Yun and P. J. Bray, "Nuclear Magnetic Resonance Studies of the Glasses in the System Na_2O-B_2O_3-SiO_2," *J. Non-Cryst. Solids*, **27**, 363–80 (1978).

[48]G. L. Turner, K. A. Smith, R. J. Kirkpatrick, and E. Oldfield, "Boron-11 Nuclear Magnetic Resonance Spectroscopic Study of Borate and Borosilicate Minerals, and a Borosilicate Glass," *J. Magn. Reson.*, **67**, 544–50 (1986).

[49]E. Oldfield, H.K.C. Timken, B. Montez, and R. Ramachandran, "High-Resolution Solid-State NMR of Quadrupolar Nuclei," *Nature (London)*, **318**, 163–65 (1985).

[50]A. C. Kunwar, G. L. Turner, and E. Oldfield, "Solid-State Spin-Echo Fourier Transform NMR of Non-Integral Spin Quadrupolar Nuclei: Observation of Undistorted Second-Order Powder Patterns for ^{39}K and ^{67}Zn Salts of High-Field," *J. Magn. Reson.*, **69**, 124–27 (1986).

[51]R. E. Taylor, R. G. Pembleton, L. M. Ryan, and B. G. Gerstein, "Combined Multiple Pulse NMR and Sample Spinning: Recovery of ^1H Chemical Shift Tensors," *J. Chem. Phys.*, **71**, 4541–45 (1979). ■